

BROADBAND FABRY–PÉROT RESONATOR FROM ZERODUR FOR LASER STABILISATION BELOW 1 KHZ LINEWIDTH WITH < 100 HZ/S DRIFT AND REDUCED SENSITIVITY TO VIBRATIONS

K.Bluss¹, A.Atvars², I.Brice², J.Alnis²¹Optek Ltd., 64 Rigas Av., Adazi, Adazi district, LV-2164, LATVIA²Institute of Atomic Physics and Spectroscopy, University of Latvia,
19 Raina Blvd., Riga, LV-1586, LATVIA

e-mail: info@optek.lv

Here we demonstrate the results of creating a two-mirror Fabry–Pérot resonator (FPR) that allows achieving the spectral width of a stabilised laser line below 1 kHz. It had low expansion Zerodur spacer and broadband high reflectance mirrors (99.85% in the range of 630 to 1140 nm). FPR was vertically mid-plane mounted for reduced sensitivity to vibrations and included in two shields inside a vacuum chamber to lower temperature fluctuations. Peltier element was used for temperature stabilisation at zero-expansion temperature. Pound–Drever–Hall (PDH) technique was applied. The signal from FPR was compared to ultra-stable signal (of about 1 Hz linewidth) to form a beat note signal. For the best performance, width of the beat note signal was below 1 kHz with the linear drift of about 23 Hz/s at 780 nm. The Allan deviation showed relative stability of the signal to be about 1×10^{-12} .

Keywords: diode laser, Fabry–Pérot resonator, narrow spectral line, optical frequency standards, PDH technique, stabilisation.

1. INTRODUCTION

For various scientific and technical applications, laser lines with stable frequencies and narrow linewidths (< 1 MHz) are needed. Fabry–Pérot resonator (FPR) is a simple tool [1] to obtain such a result even from semi-stable lasers with rather broad lines (for diode laser spectral linewidth typically is about 10–50 MHz). Main parts of FPR are two parallel mirrors separated with a certain distance L . In this distance, a laser light can form its standing wave modes with narrow spectral width (typically of about 50 kHz). These modes can become forming elements for a reflected narrow linewidth of a laser line. Due to the change of distance between mirrors of FPR (typically because of vibrations and temperature change), its narrow resonance mode is jittering and drifting and, thus, the final averaged linewidth of a laser light becomes larger. To make the final linewidth of a laser line narrower, various techniques are used to minimise the vibration and temperature change of FPR. For vibration damping special platforms are used, resonators are made in shapes that are less sensitive to vibration (first there were schemes with horizontal FPR mount

[2], then with vertical FPR mount [3], spherical mount [4] and cubic mount [5]). To minimise temperature change [6], spacers for FPR are made of low expansion materials (for example, of ULE glass or Zerodur material), FPR is put into thermal shields, Peltier elements are used to cool and heat the FPR, temperature sensors are used for the control. Additionally, FPR is installed into a vacuum chamber. This allows reducing fluctuations of optical length of laser light in FPR due to fluctuations of a refractive index of gas (refraction index of gas fluctuates as the pressure fluctuates). Even with the most advanced techniques to minimise the vibration and temperature change of FPR, the material of spacers of FPR (as all other material) experiences thermal noise and this effect gives the theoretically calculated stability of FPR of about 0.1 Hz [7], [8]. Additionally, the frequency of laser line experiences jitter due to processes within the laser itself (because of temperature and current changes); therefore, various loop techniques are used to stabilise the frequency (for example, Pound–Drever–Hall technique [9], [10]). **Currently, a well-performed vertical FPR with advanced techniques for vibration damping and temperature change minimisation gives a linewidth of about 0.5 Hz and a frequency drift of 0.1 Hz/s [6].** Such parameters of laser line are necessary for ultra-precise measurements, for example, for atomic clocks [11] and the determination of the change of the gravitation constant [12].

The current paper focuses on the scheme of a vertical FPR and measurement technique that gives a linewidth of 1 kHz and a frequency drift < 100 Hz/s of a diode laser line. These parameters are not the best available to achieve, but are sufficient for various applications where narrow laser lines are needed, for example, for ion trap experiments [13], for research on whispering gallery mode resonators [14], for laser cooling [15], for research on Rydberg atoms [16], and for research in molecular spectroscopy [17].

FPR is a rather cheap tool to stabilise a laser line. However, there are several other techniques for stabilisation, for example, frequency combs [18].

2. EXPERIMENT

Here we present experimental equipment and special construction of FPR that allowed us to reach the stability of the laser line of about 1 kHz. As a light source, the laser diode Sanyo DL7140-201S (wavelength 785 ± 10 nm, optical output power 70 mW) was used in an external cavity configuration with a diffraction grating [19]. The light was sent to a vertical FPR through optical fibre. Pound–Drever–Hall (PDH) technique [9], [20], [21] was used for laser stabilisation to FPR line.

A. Construction of a Resonator

To reach a significant stability of a laser line, various tricks were employed in the construction of the FPR shown in Fig. 1.

It should be mentioned that the stability of the FPR is dependent on the stability between two mirrors (M) of FPR. All factors that can change the distance between these mirrors have to be minimised. The first source for the distance change is

mechanical vibrations. Activities for minimising vibrations have to be implemented. At first, the FPR has to be put on a stable optical table with air dampers. Then the vertical FPR mid-plane construction is selected (other alternatives are horizontal and spherical constructions). FPR is put inside the heat shield (HS2) and is held with nylon plastic screws (PS) without touching walls. The second source is the change of the distance due to thermal expansion of materials. Therefore, the low-expansion Zerodur material (in the range of 0°C to 50°C it has an expansion coefficient up to $\pm 0.007 \times 10^{-6}/\text{K}$ that is two orders of magnitude better than that of fused quartz) is used as a spacer (in the form of a drilled-through cylinder (GT), length 120 mm, diameter 50 mm, diameter of the borehole 20 mm). Optical cavity is surrounded with two heat shields and placed inside a vacuum chamber to minimise temperature fluctuations. Temperature of the outer heat shield HS1 is actively stabilised with a double-stage Peltier element. Temperature sensor TS1 is used for regulation and is placed close to the Peltier element and thermally coupled to the inner heat shield HS2 allowing one to maintain the temperature stability of the resonator within a few mK. In external heat shield (HS1), special holes (HH) are drilled for inner and outer low vacuum regions to be joined and yet not to be influenced by thermal infrared radiation. The third source of the change of distance between mirrors is pressure fluctuation of the gas inside FPR. Therefore, inside the resonator vacuum is obtained. Vacuum chamber is assembled from CF-type ultra-high vacuum chamber parts. Two-vacuum pump system is used – a turbomolecular vacuum pump for pre-evacuation and an ion getter vacuum pump running continuously for maintaining high vacuum below 1×10^{-5} mbar.

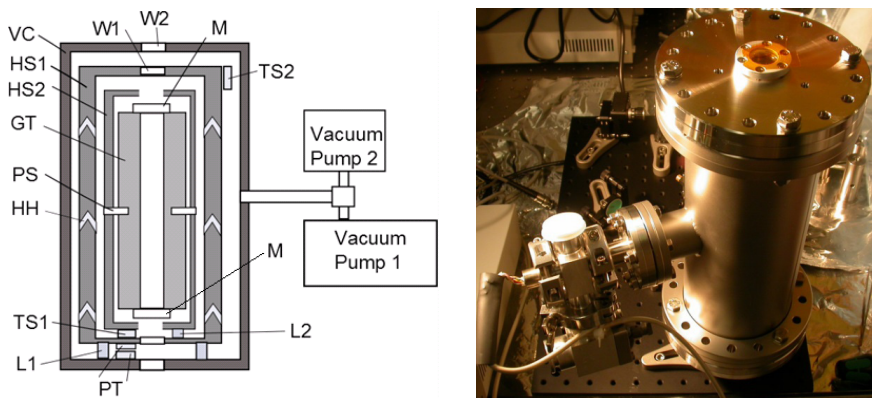


Fig. 1. Left: Drawing of the FPR assembly. VC – a vacuum chamber, HS1 and HS2 – aluminium heat shields, GT – the Zerodur glass cylinder with a central hole, PS – plastic screws, HH – holes with thermal radiation blocking, TS1 and TS2 – temperature sensors, L1 and L2 – mechanical legs, PT – two-stage Peltier element, W1 and W2 – windows with antireflection coating, M – cavity mirrors. Right: photo of the assembled FPR.

For resonator universality, mirrors (M) with high optical reflectance in broad optical region were used (for the spectral range of 630–1140 nm reflectance is achieved above 99.85%, *LAYERTEC*, No. 103521, R.o.c. = 1 m). Such mirrors are used for femtosecond Ti:Sa laser and are off-the-shelf components.

B. Experimental Scheme

Principal scheme for the experimental equipment is given in Fig. 2.

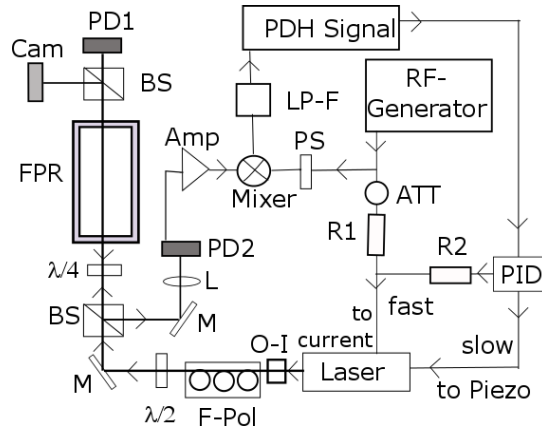


Fig. 2. Principal schema of experimental equipment. O-I – an optical isolator, F-Pol – a fibre polariser, $\lambda/2$ plate, M – a mirror, BS – a beam splitter, $\lambda/4$ plate, FPR – the Fabry-Pérot resonator, PD1, PD2 – photodiodes, Cam – a video camera, L – an optical lens, Amp – an amplifier, Mixer – a signal mixer, PS – a phase shifter, LP-F – a low-pass filter, PDH Signal – the Pound-Drever-Hall error signal, RF-Generator – a radio frequency modulation generator, ATT – an attenuator, R1 and R2 – electric resistors, PID – the PID controller. Fast part of the feedback loop signal goes into current of a laser; slow part of the signal goes into the Piezo element of the laser.

The path of the signal in the experimental schema is the following: a signal comes from the laser into an optical isolator (O-I). External cavity diode laser was custom built and had no internal isolator. It prohibits the signal from travelling back into the laser (that may occur due to various reflections). Then the signal goes into the fibre which forms a Fibre Polariser (F-Pol) that can change the polarisation of a signal to obtain linearly polarised light beam. $\lambda/2$ plate is used to align the polarisation vector of the light. The transmitted light through the FPR has the same polarisation as the incident light and goes into beamsplitter (BS) which gives the signal to a video camera (Cam) that is used during the alignment of a laser beam into FPR to assure that resonator mode TEM_{00} is excited. Photodiode PD1 is used to monitor the transmitted light. The reflected light from FPR has the opposite circular polarisation compared to incident light. To extract reflected light from the FPR for obtaining the PDH error signal $\lambda/4$ plate and a polarising beam splitter cube are used. $\lambda/4$ before the FPR changes the linear polarisation of light to circular polarisation. Light reflected from the resonator passes $\lambda/4$ again and becomes orthogonally polarised in respect to the incoming light and is reflected sideways by a polarising beam splitter cube (BS), directed by mirror M, and focused by lens (L) on the photodiode (PD2). Now the signal is electrical. Signal is amplified (Amp) and goes into the Mixer. Here the signal is mixed with the radio frequency modulation signal obtained from RF-Generator. Phase shifter (PS) is used to align signals of PD2 and RF-Generator. Then the signal goes through a low-pass filter (LP-F) and here the PDH error signal is obtained (PHD Signal). This signal goes back to the laser by two channels after the proportional integral derivative PID controller. Slow frequency channel goes into Piezo crystal of

laser and is used to modulate the path of laser resonator, but a fast frequency channel goes through resistor R2 and meets with RF-Generator modulation signal previously transmitted through an attenuator (ATT) and goes through resistor R1. The sum signal goes into the laser diode to modulate the current of the laser.

Then the laser light signal is optically mixed with another signal from the ultra-stable laser (with a line width of 0.5 Hz and frequency drift of 0.1 Hz/s [6]) to form a beat note signal (not shown in Fig. 2). The modulation radio frequency was about 7 MHz. To make the resonator assembly usable in a broad colour range, we used broadband anti-reflection coated optics (Thorlabs coating 650–1050 nm) and achromatic λ – plates.

3. RESULTS AND DISCUSSION

Various standard measurements were performed during the test of the equipment – measurement of the reflected signal of FPR, measurement of the PDH signal, measurement of the beat note signal, measurement of the wide spectra and narrow spectra. Calculations were done to obtain the Allan deviation from the beat note signal.

C. Measurements of Beat Note Signals

Beat note signal of the laser signal from the developed equipment and from the ultra-stable laser was observed. Figure 3 shows the beat note signal when the vibration damping of the optical table is activated. The width of beat note signal is about 1 kHz. Figure 3 is **only a snapshot of the signal – the actual signal changes during the time – peak frequencies change their position, yet the width of the fluctuating signal still remains in the range of approximately 1 kHz.** Without vibration damping of the optical table, the beat note is broadened to approximately 10 kHz.

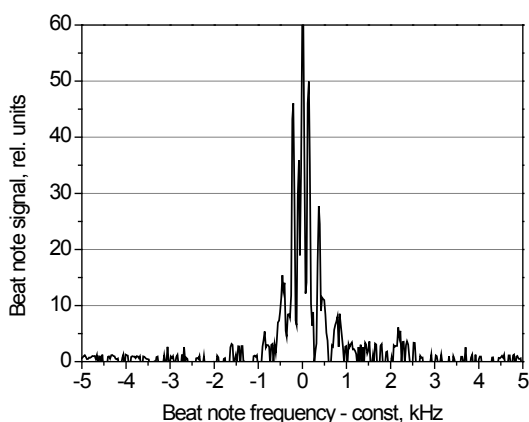


Fig. 3. Beat note signal of the FPR stabilised by the PDH technique, with vibration damping of the optical table. The signal shows full width at half maximum of about 1 kHz. Resolution bandwidth of FFT analyser used was 200 Hz.

D. Measurements of the Beat Note Signal versus Time

The beat note signal drift with the time is shown in Fig. 4. This shows that the signal is fluctuating and is experiencing the linear drift of about 120 Hz/s (the first week of operation). The drift can be decreased by optimising the temperature of the system to the lowest thermal expansion region of Zerodur. The search for an optimal temperature is described in Section D. When the optimal temperature is selected the drift can be minimised to 23 Hz/s (Fig. 4 – the right side).

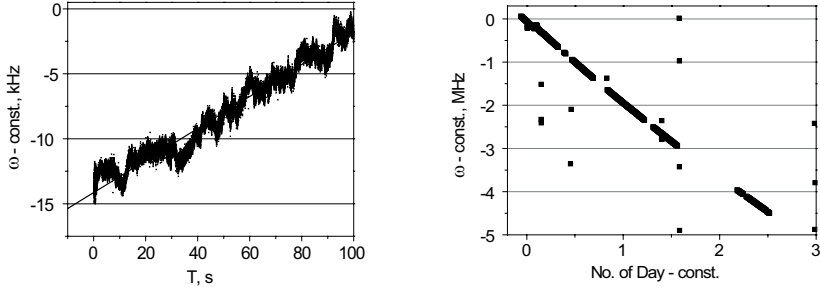


Fig. 4. The typical beat note signal as dependent on time. Left: a short-term fluctuating beat note signal that experiences the linear drift of about 120 Hz/s. Right: a long-term beat note signal with a linear drift of about 23 Hz/s.

E. Calculation of the Allan Deviation

From the dependence of the beat note signal on the time, the Allan deviation can be calculated [22]–[24]. The plot of Allan deviation with good characteristics achieved for FPR is seen in Fig. 5. Here we see that the Allan deviation remains between 0.1–0.6 kHz when linear drift of 70 Hz/s is removed. For a diode laser wavelength used in the experiment $\lambda_0 = 780 \text{ nm}$, the frequency is about $3.8 \times 10^{14} \text{ Hz}$. The relative stability of the frequency of the system seen from the Allan deviation is about 1×10^{-12} .

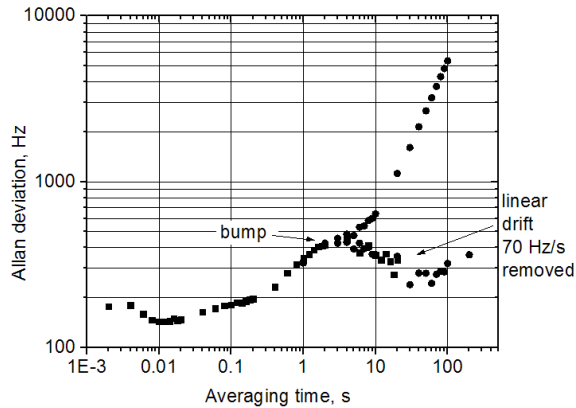


Fig. 5. Allan deviation of a beat signal. Here we see linear drift of about 70 Hz/s after 1 s. When the linear drift is subtracted, then the Allan deviation remains between 0.1–0.6 kHz at optical frequency of $3.8 \times 10^{14} \text{ Hz}$ (780 nm).

The bump in the Allan deviation graph at about 1 s can be explained by the presence of parasitic reflections between laser and FPR. This corresponds to 1 Hz resonance of air fluctuations [25]. Optical isolator (O-I in Fig. 2) was used to prevent the entrance of parasitic reflections back into laser. In this experiment, the available optical isolator was used. However, as it was designed for the central wavelength of 980 nm, isolation was not complete. For a better performance, a two-stage (60dB) optical isolator should be used.

F. Optimal Temperature Selection

Zerodur material possesses a temperature where a thermal expansion coefficient is crossing zero, but the exact temperature depends on manufacturing conditions. To achieve better results for the stability of the beat note signal, the optimal temperature of FPR can be estimated and maintained. A search was made (Fig. 6) by daily changing the temperature of the system and measuring the beat note signal. It was found that the smallest resonator drift response to a temperature change appeared at the temperature of about $T_c=27.6(1)^\circ\text{C}$.

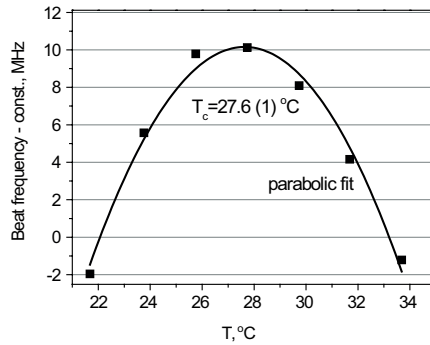


Fig. 6. Measured (dots) and fit (line) beat note frequency corresponding to the temperature of the FPR. To minimise the effect on temperature sensitivity, the FPR temperature has to be stabilised on the maximum of a curve occurring at $T_c = 27.6(1)^\circ\text{C}$.

G. Minimising the Long-term Linear Drift

Additional beat note measurements were made to observe the long-term drift if the temperature of FPR is remaining stable. It was observed that in the first days of continuous operation the drift of the FPR line decreased from 70 Hz/s to 35 Hz/s. Therefore, it seems that the system works better when it operates for a longer time. Such behaviour is observed in hydrogen maser clocks where it takes about a month for the resonator to reach the best stability [26]. For the system to operate for several days or months, the UPS power supply is installed to protect against abrupt power failures.

There are several effects causing continuous FPR drift [8], [27]: aging of the material, the settling of the optical contacts of mirrors, aging of the temperature

control, the decrease of the manufacturing mechanical stress of the spacer, shrinking of glass-ceramics (for Zerodur $\Delta L/L \approx 2 \cdot 10^{-15}/s \sim 5$ Hz/s), ongoing crystallisation of the glass phase, $\Delta L/L \approx 1 \cdot 10^{-16}/s \sim 0.4$ Hz/s).

4. CONCLUSIONS

The current paper shows the construction of Fabry–Pérot resonator and the measurement scheme that allows reaching the frequency stabilisation of the laser signal below 1 kHz and a frequency drift of about 23 Hz/s at 780 nm. The device is transportable. Application wavelengths are in the range of 630–1140 nm with the reflectance of mirrors above 99.85%. From the construction point of view, the current FPR is not much worse than the construction shown in [6] and giving 1 Hz spectral width. The difference is that mirrors here had a lower reflectance index than those used in [6], but the spectral region of high reflectance is much broader allowing one to use the same resonator for experiments with lasers of different colours. Additional improvements can be made for next construction of similar resonators, for example, spacer material from Zerodur can be changed to ULE material (now ULE is becoming increasingly popular with the drop of its price), and electronics of the temperature controller can be placed right into the vacuum chamber. The current system and Fabry–Pérot resonator were made as small budget devices for use in various applications in a wide spectral region.

ACKNOWLEDGEMENTS

The research has been supported by the European Regional Development Fund within the project “Competence Centre of Latvian Electronic and Optical Equipment Production”, individual research project No. 1.4., programme “Entrepreneurship and Innovations” Appendix 2.1.2.1.1. activity “Centres of Competence”, contract No. L-KC-11-0006.

We thank the group led by Prof. Theodor Hänsch at the MPQ Garching for an opportunity to carry out measurements against an ultra-stable laser.

REFERENCES

1. Demtröder, W. (2008). *Laser Spectroscopy*. Berlin, Heidelberg: Springer Berlin Heidelberg. doi:10.1007/978-3-540-73418-5
2. Webster, S., Oxborrow, M., & Gill, P. (2007). Vibration insensitive optical cavity. *Physical Review A*, 75(1), 011801. doi:10.1103/PhysRevA.75.011801
3. Matveev, A. N., Kolachevsky, N. N., Alnis, J., & Hänsch, T. W. (2008). Semiconductor laser with the subhertz linewidth. *Quantum Electronics*, 38(10), 895–902. doi:10.1070/QE2008v038n10ABEH013806
4. Leibrandt, D. R., Thorpe, M. J., Notcutt, M., Drullinger, R. E., Rosenband, T., & Bergquist, J. C. (2011). Spherical reference cavities for frequency stabilization of lasers in non-laboratory environments. *Optics Express*, 19(4), 3471–82. doi:10.1364/OE.19.003471
5. Webster, S., & Gill, P. (2011). Force-insensitive optical cavity. *Optics Letters*, 36(18), 3572–4. doi:10.1364/OL.36.003572

6. Alnis, J., Matveev, A., Kolachevsky, N., Udem, T., & Hänsch, T. W. (2008). Subhertz line-width diode lasers by stabilization to vibrationally and thermally compensated ultralow-expansion glass Fabry-Pérot cavities. *Physical Review A*, *77*(5), 053809. doi:10.1103/PhysRevA.77.053809
7. Numata, K., Kemery, A., & Camp, J. (2004). Thermal-Noise Limit in the Frequency Stabilization of Lasers with Rigid Cavities. *Physical Review Letters*, *93*(25), 250602. doi:10.1103/PhysRevLett.93.250602
8. Kessler, T., Legero, T., & Sterr, U. (2011). Thermal noise in optical cavities revisited. *Journal of the Optical Society of America B*, *29*(1), 178. doi:10.1364/JOSAB.29.000178
9. Drever, R. W. P., Hall, J. L., Kowalski, F. V., Hough, J., Ford, G. M., Munley, A. J., & Ward, H. (1983). Laser phase and frequency stabilization using an optical resonator. *Applied Physics B Photophysics and Laser Chemistry*, *31*(2), 97–105. doi:10.1007/BF00702605
10. Black, E. D. (2001). An introduction to Pound–Drever–Hall laser frequency stabilization. *American Journal of Physics*, *69*(1), 79. doi:10.1119/1.1286663
11. Bloom, B. J., Nicholson, T. L., Williams, J. R., Campbell, S. L., Bishof, M., Zhang, X., Zhang, W., Bromley, S.L, Ye, J. (2014). An optical lattice clock with accuracy and stability at the 10(-18) level. *Nature*, *506*(7486), 71–5. doi:10.1038/nature12941
12. Yu, Y., Mitryk, S., & Mueller, G. (2014). Arm locking for space-based laser interferometry gravitational wave observatories. *Physical Review D*, *90*(6), 062005. doi:10.1103/PhysRevD.90.062005
13. Batteiger, V., Knünz, S., Herrmann, M., Saathoff, G., Schüssler, H., Bernhardt, B., Wilken, T., Holzwarth, R., Hänsch, T.W., Udem, T. (2009). Precision spectroscopy of the 3s-3p fine-structure doublet in Mg⁺. *Physical Review A*, *80*(2), 022503. doi:10.1103/PhysRevA.80.022503
14. Fescenko, I., Alnis, J., Schliesser, A., Wang, C. Y., Kippenberg, T. J., & Hänsch, T. W. (2012). Dual-mode temperature compensation technique for laser stabilization to a crystalline whispering gallery mode resonator. *Optics Express*, *20*(17), 19185–93.
15. Sesko, D., Fan, C. G., & Wieman, C. E. (1988). Production of a cold atomic vapor using diode-laser cooling. *Journal of the Optical Society of America B*.
16. Oxley, P., & Collins, P. (2010). Frequency stabilization of multiple lasers and Rydberg atom spectroscopy. *Applied Physics B*, *101*(1-2), 23–31. doi:10.1007/s00340-010-4154-z
17. Dinesan, H., Fasci, E., Castrillo, A., & Gianfrani, L. (2014). Absolute frequency stabilization of an extended-cavity diode laser by means of noise-immune cavity-enhanced optical heterodyne molecular spectroscopy. *Optics Letters*, *39*(7), 2198–201. doi:10.1364/OL.39.00219
18. Cundiff, S. T., & Ye, J. (2005). *Femtosecond Optical Frequency Comb: Principle, Operation, and Applications*. Boston: Springer. doi:10.1007/b102450
19. Wieman, C. E., & Hollberg, L. (1991). Using diode lasers for atomic physics. *Review of Scientific Instruments*, *62*(1), 1–20. doi:10.1063/1.1142305
20. Izumi, K., Sigg, D., & Barsotti, L. (2014). Self-amplified lock of an ultra-narrow line-width optical cavity. *Optics Letters*, *39*(18), 5285. doi:10.1364/OL.39.005285
21. Zhu, M., Wei, H., Wu, X., & Li, Y. (2015). Fabry-Pérot interferometer with picometer resolution referenced to an optical frequency comb. *Optics and Lasers in Engineering*, *67*, 128–134. doi:10.1016/j.optlaseng.2014.11.010
22. Riehle, F. (2003). *Frequency Standards*. Weinheim, FRG: Wiley-VCH Verlag GmbH & Co. KGaA. doi:10.1002/3527605991
23. Allan, D. W. (1966). Statistics of atomic frequency standards. *Proc. IEEE*, *54*, 221–230.

24. Rutman, J. (1978). Characterization of phase and frequency instabilities in precision frequency sources: Fifteen years of progress. *Proceedings of the IEEE*, 66(9), 1048–1075. doi:10.1109/PROC.1978.11080
25. Melikov, A. K., Krüger, U., Zhou, G., Madsen, T. L., & Langkilde, G. (1997). Air temperature fluctuations in rooms. *Building and Environment*, 32(2), 101–114.
26. Private communication of J.A. with hydrogen maser CH1-75A manufacturer Quartz-lock.
27. Sterr, U., Legero, T., Kessler, T., Schnatz, H., Grosche, G., Terra, O., & Riehle, F. (2009). Ultrastable lasers – new developments and applications. *Proc. of SPIE*, 7431, 74310A–14. doi:10.1117/12.825217

PLATJOSLAS FABRĪ-PERO REZONATORS NO ZERODUR
MATERIĀLA LĀZERA STABILIZĀCIJAI ZEM 1 KHZ
SPEKTRĀLĀ PLATUMA AR < 100 HZ/S ILGTERMIŅA
DREIFU UN SAMAZINĀTU VIBRĀCIJU
JUTĪGUMU

K. Blušs, A. Atvars, I. Brice, J. Alnis

K o p s a v i l k u m s

Dotajā rakstā demonstrēta divu spoguļu Fabrī-Pero rezonatora (FPR) konstrukcija un eksperimentālā shēma, kura ļauj iegūt stabilizēta lāzera līnijas platumu mazāku nekā 1 kHz. FPR spoguļi bija ar platu augstas atstarošanas joslu (99.85% atstarošana viļņu garumu intervālā 630 līdz 1140 nm) un starplika starptiem bija izveidota no Zerodur materiāla. Lai mazinātu vibrāciju ietekmi, FPR tika stiprināts vertikāli pusaugstuma plaknē. Lai mazinātu temperatūras fluktuācijas, rezonators tika ietverts 2 apvalkos vakuuma kamerā. Peltjē elementi tika izmantoti temperatūras stabilizēšanai pie starplikas materiāla nulles izplešanās temperatūras. Lāzera piesaistei pie FPR rezonanses tika pielietota Pound-Drever-Hall metode. Signāls no FPR tika salīdzināts ar ultra-stabilu optisko signālu (ar līnijas platumu ap 1 Hz), kopā veidojot interferences sitienu signālu. Labākie iegūtie signāli parādīja, ka FPR nodrošina lāzera līnijas stabilizāciju zemāku kā 1 kHz un lineāro dreifu ap 23 Hz/s pie viļņa garuma 780 nm. Alana deviācija rādīja, ka signāla frekvences relatīvā stabilitāte ir ap 1×10^{-12} .

16.04.2015.